SIGNATURE OF INCOMPLETE FUSION IN THE α-CHANNELS OF ^{6}Li + ^{93}Nb REACTION*

Ankur Singh, Moumita Maiti†

Department of Physics, Indian Institute of Technology Roorkee
Roorkee — 247667, Uttarakhand, India

Received 6 November 2023, accepted 23 December 2023, published online 24 April 2024

The article discusses the underlying reaction dynamics in the ^{6}Li+^{93}Nb reaction through the excitation function analysis within the 24–43 MeV energy domain employing an activation technique followed by off-beam γ-spectroscopy. The comparison of measured data with equilibrium and preequilibrium-based statistical model calculations implies a fair reproduction of n-channel data by the EMPIRE EGSM level density predictions, suggesting the production of Ru radionuclides via the complete fusion mechanism. The enhancement in α-channel cross sections relative to the theory is evident of competing incomplete fusion (ICF) process owing to the weak binding of the ^{6}Li projectile. The estimated ICF strength fraction from the α-channels obeys an increasing trend with incident energy.

DOI:10.5506/APhysPolBSupp.17.3-A27

1. Introduction

The cluster structure $(\alpha + x)$ of weakly bound nuclei emanates manifold reaction mechanisms such as a direct breakup, elastic breakup, transfer followed by a breakup, and nucleon transfer in addition to dominant complete fusion (CF) [1]. Breakup phenomena have been investigated extensively using the continuum discretized coupled channel approach [2–4]. The reduction in fusion cross sections (relative to one-dimensional barrier penetration model calculations) implied by the loss in incident flux owing to projectile breakup has been realized at the above barrier energies [1, 5]. In-beam measurement studies suggest the prompt breakup as well as the transfer followed by the breakup of the ^{6}Li projectile [2]; while the prompt breakup of ^{6}Li is found to dominate over the other as in Ref. [6], contrary to Ref. [2]. An apparent enhancement in p- and/or α-channel residual cross

* Presented at the XXXVII Mazurian Lakes Conference on Physics, Piaski, Poland, 3–9 September, 2023.

† Corresponding author: moumita.maiti@ph.iitr.ac.in

sections relative to CF-based model predictions has been perceived as the signature of incomplete fusion (ICF) [7, 8]. Distinct experimental techniques such as offline γ-spectroscopy, time of flight method, spin distribution, and recoil range distribution have been investigated to put forth a concrete picture of ICF over the years. However, several ambiguities are prevalent in systematic studies, such as the unknown onset of ICF in low-energy reactions, ambiguous entrance channel dependencies, and no universal trend of fusion suppression due to breakup. Likewise, a few studies [8] suggest an increasing trend of ICF strength fraction (F_{ICF}) with entrance channel parameters, while others [9, 10] report an exponential or monotonic behavior. Reference [11] suggests an increasing trend of fusion suppression with the Coulomb factor, contrary to that of independency indicated in Ref. [12]. In order to address the ambiguities, more focused efforts are needed to scrutinize reaction dynamics over the entire mass domain. The present study, which discusses the breakup fusion strength in α-emitting channels from the ^{6}Li $+^{93}$ Nb reaction, has delivered an extended endeavor to address the ambiguous findings.

2. Experimental methodology

$^{6}Li^{+3}$ ion beam in the energy range of 24–43 MeV was bombarded on the stacks of 1.3–2.2 mg/cm^2 thick Nb foils interspersed with 1.5–1.8 mg/cm^2 thick Al foils at the BARC-TIFR pelletron facility, Mumbai, India. The time-invariant average beam current and beam flux were $\sim$ 9.4 pnA and $\sim 5.8 \times 10^{10}$ particles/sec, respectively. The energy points in the excitation functions (EFs) represent the average of energies entering and leaving a target foil. The SRIM code was used to compute the degradation of energy at successive target-catcher foils. Post irradiation, the induced residual activity was registered using a precalibrated HPGe detector having a resolution of $\leq$ 2 keV at 1332 keV of ^{60}Co. The data were acquired using the multichannel analyzer coupled to a PC operating with the GENIE2k software. The radionuclides were identified from their unique γ-emissions and experimental decay profiles. The residual cross sections were estimated using the standard activation formula [7]. The measured data have uncertainty from factors such as statistical error in photo-peak area, target thickness ($\sim$ 2%), beam flux ($\sim$ 5–7%), and detector efficiency ($<$ 2%). The energy uncertainty has contributions from the SRIM calculation and energy loss at each target foil.

3. Results and discussion

Analysis of the acquired γ-spectra from residual activity ensured the population of ^{95,94}Ru, ^{93m}Mo, and ^{92m}Nb radionuclides via xn ($x = 4, 5$), $\alpha 2n$, and $\alpha p 2n$ channels, respectively, in the ^{6}Li $+^{93}$ Nb reaction. The

measurement was taken at above barrier energies within the 24–43 MeV energy range. The barrier parameters of the system obtained by fitting the measured fusion data (sum of residual cross sections contributing to CF) using Wong's formalism [13] are barrier height $V_B = 19.1 \pm 2.8$ MeV and barrier radius $R_B = 8.9 \pm 0.4$ fm. The extracted barrier parameters are in close proximity (within errors) to the parameters $V_B = 17.5$ MeV and $R_B = 9.3$ fm from the Bass systematics [14], thus validating the measured data. The comprehensive analysis of the residues is presented in the framework of theoretical predictions from the statistical model codes EMPIRE3.2.2 [15] and ALICE23 [16] to understand the strength of mechanisms feeding their production. Both codes predict the residual cross sections by considering the equilibrium (EQ) and preequilibrium (PEQ) as fundamental mechanisms. EMPIRE employs the Hauser–Feshbach formalism for EQ, while ALICE adopts the Weisskopf–Ewing model for EQ. The exciton model simulates the PEQ emissions in the EMPIRE code, while a Monte Carlo-based Hybrid or Geometry-dependent Hybrid model accounts for PEQ in the ALICE code. Phenomenological models such as the Gilbert–Cameron (GC) model and enhanced generalized superfluid model (EGSM) are adopted for level density in the EMPIRE code, while ALICE considers the Fermi gas (FG) model and the Kataria–Ramamurthy (KR) model. A detailed description of the model codes can be found elsewhere [7, 8].

***n*-channel:** ^{6}Li fusion with ^{93}Nb forms the ^{99}Ru* compound nucleus, which populates the Ru isotopes on deexcitation via different neutron channels. Figure 1 (a) displays the measured cumulative residual cross sections from neutron channels, $\Sigma\sigma_{xn}$ ($x = 4, 5$) examined comparatively with theoretical predictions from the EMPIRE and ALICE codes. One may notice that EMPIRE has reasonably reproduced the measured data ($\Sigma\sigma_{xn}$) with EGSM level density, while EMPIRE with GC thoroughly overestimates the data. ALICE with KR also explains the low-energy data up to 32.6 MeV, followed by an overestimation at higher energies. ALICE FG calculations could justify a lower energy point, while a gradual deviation can be seen for subsequent energy points. EMPIRE predicts the residual cross sections in the framework of CF dynamics, a reasonable description of measured neutron channel data by EMPIRE with EGSM, therefore, hints at the population of ^{95,94}Ru radionuclides via the CF process. Furthermore, EMPIRE with EGSM is regarded as the optimum calculation in interpreting the role of mechanisms prevalent in subsequent channels.

α-channel: From α-emitting channels, we could identify two residues, namely, ^{93m}Mo ($\alpha 2n$-channel) and ^{92m}Nb ($\alpha p2n$-channel). The comparative analysis of measured EFs of these residues with optimum calculation (EMPIRE with EGSM) revealed a considerable enhancement, which is exhibited by the measured cumulative data ($\Sigma\sigma_{\alpha(2n,p2n)}$) reported in Fig. 1 (b).

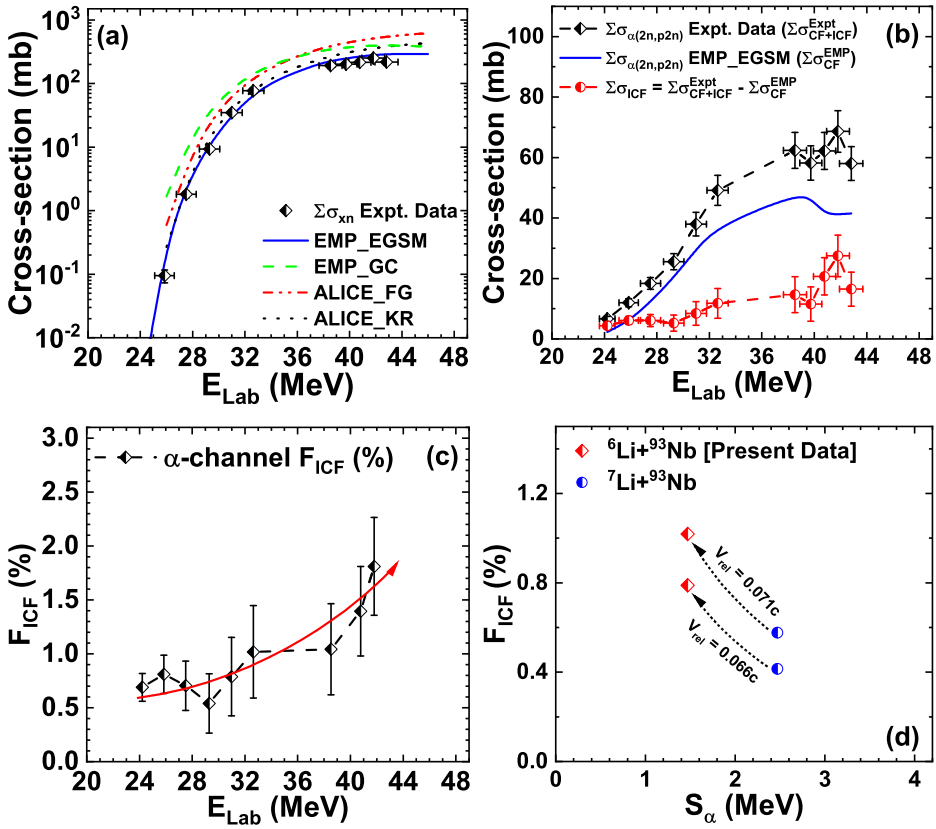

Fig. 1. (a) Comparison of measured cumulative n-channel data ($\Sigma\sigma_{xn}$) with theoretical estimations from EMPIRE with EGSM (solid curve), GC (dashed curve) level densities, and ALICE with FG (dash-double-dotted curve), KR (dotted curve) level densities. (b) Comparison of measured cumulative α-channel data ($\Sigma\sigma_{\alpha(2n,p2n)}$) with optimum EMPIRE EGSM estimates. Deduced ICF cross sections have also been reported. The line joining the symbols is to guide the eyes. (c) Variation of α-channel $F_{\rm ICF}$ with bombarding energy. (d) Comparison of α-channel $F_{\rm ICF}$ for the ^{6}Li + ^{93}Nb and ^{7}Li + ^{93}Nb [8] systems as a function of α-separation energy of the projectile at two distinct $V_{\rm rel}$.

The enhancement in measured α-channel data relative to theory in weakly bound projectile-induced reactions is an apparent sign of the breakup fusion mechanism in conjunction with CF due to the low breakup threshold of ^{6}Li, as suggested in the literature [7, 8, 17].

In view of the enhancement observed in α-channels of the ^{6}Li+^{93}Nb reaction, the role of ICF has been perceived in feeding the production of α-channel radionuclides besides the CF mechanism. In the CF process, the

^{6}Li projectile completely merges with the ^{93}Nb target at once and forms a composite system, which on equilibration, yields a ^{99}Ru* compound nucleus in the excited state. The ^{99}Ru* subsequently deexcites via distinct channels to form the residues measured in the present study. The population of residues kinematically depends on the excitation energy of the compound nucleus and the reaction threshold. One may readily infer the population of residues via the CF process from the channel thresholds (Table 1) being lesser than the excitation energy (E^{*} = 37.3–54.7 MeV within the studied energy domain) of the compound nucleus. In the ICF process, owing to the low breakup threshold, ^{6}Li may get ruptured into two fragments α+d. Fusion of either α or d with ^{93}Nb (with the second fragment d or α flying away as a spectator) may yield a reduced compound nucleus ^{97}Tc* or ^{95}Mo*, which on deexcitation via distinct channels may populate ^{93m}Mo and ^{92m}Nb residues. Thus, we observe the enhanced experimental cross sections relative to the theory, which only considers the CF dynamics. The population of these residues via α-ICF or d-ICF may be inferred from the reaction energetics (Table 1) as the excitation energy of reduced compound nuclei, E^{*} = 17–28.9 MeV for ^{97}Tc* in α-ICF or E^{*} = 21–27.1 MeV for ^{95}Mo* in d-ICF within the studied energy domain, is larger than the respective reaction thresholds. The reaction thresholds for d-ICF being much lower than α-ICF suggest the domination of d-capture over α-capture by the target [5, 17]. Besides the prompt breakup of ^{6}Li, transfer followed by breakup channels (α+p or α+α) may also feed the ICF mechanism [17]. However, Ref. [3] reports a significant contribution from the prompt breakup process over others. Furthermore, using the present technique, one cannot experimentally disentangle the prompt breakup and transfer followed by breakup processes. The data reduction method [8, 17] has been employed to quantify the α-channel ICF contribution in the reaction using the relation $\Sigma\sigma_{\mathrm{ICF}} = \Sigma\sigma^{\mathrm{Expt}}_{\mathrm{CF+ICF}} - \Sigma\sigma^{\mathrm{EMP}}_{\mathrm{CF}}$, where $\Sigma\sigma^{\mathrm{Expt}}_{\mathrm{CF+ICF}}$ is the sum of measured data of α-channels and $\Sigma\sigma^{\mathrm{EMP}}_{\mathrm{CF}}$ is the sum of theoretical cross sections of the same channels, as reported in Fig. 1 (b). One may notice that the rela-

Table 1. Production of residues via CF and ICF channels and corresponding reaction thresholds.

CF of ^{6}Li	E_{th} [MeV]	ICF of ^{6}Li	E_{th} [MeV]
^{93}Nb(^{6}Li,4n)^{95}Ru	23.2	^{93}Nb(α,tn)^{93m}Mo	21.7
^{93}Nb(^{6}Li,5n)^{94}Ru	32.7	^{93}Nb(α,αn)^{92m}Nb	9.1
^{93}Nb(^{6}Li,α2n)^{93m}Mo	5.1	^{93}Nb(d,2n)^{93m}Mo	3.4
^{93}Nb(^{6}Li,αp2n)^{92m}Nb	13.2	^{93}Nb(d,t)^{92m}Nb	2.6

tive separation of experimental data and theoretical estimates increases with rising projectile energy, indicating the enhanced breakup probability of ^{6}Li with energy as shown by deduced ICF cross sections in Fig. 1 (b). The α-channel ICF strength fraction, defined as $F_{\rm ICF} = \Sigma\sigma_{\rm ICF}/\sigma_{\rm TF}^{\rm th}$, where $\Sigma\sigma_{\rm ICF}$ is the deduced α-channel ICF cross section and $\sigma_{\rm TF}^{\rm th}$ is the theoretical total fusion cross section, also obeys an increasing trend with bombarding energy (Fig. 1 (c)) in consonance with earlier measurements [8]. It should be noted that the reported α-channel ICF may be regarded as the lower limit owing to the unaccounted missing channels (short-lived or stable residues) that could not be measured using the present technique. To emphasize the role of projectile structure in reaction dynamics, we have compared the α-channel $F_{\rm ICF}$ from ^{6}Li and ^{7}Li [8] reactions on ^{93}Nb at different relative velocities *viz.* $V_{\rm rel} = 0.066$c and 0.071c in Fig. 1 (d). Evidently, owing to the larger breakup threshold for ^{7}Li ($S_\alpha = 2.47$ MeV) than ^{6}Li ($S_\alpha = 1.47$ MeV), we have estimated the smaller α-channel $F_{\rm ICF}$ for ^{7}Li reaction over ^{6}Li reaction. Thus, it may be concluded that the projectiles having a lower breakup threshold may yield larger ICF for reactions involving the same target. Larger $F_{\rm ICF}$ values at $V_{\rm rel} = 0.071$c compared to $V_{\rm rel} = 0.066$c indicate the role of bombarding energy.

4. Conclusion

The measured cumulative cross sections of n- and α-channel residues from the ^{6}Li+^{93}Nb reaction have been reported within the 24–43 MeV energy region. EF analysis in the framework of the EMPIRE and ALICE codes puts forth EMPIRE with EGSM being favorable in reproducing the neutron channel data. Thus, the predominant role of the CF mechanism has been interpreted in feeding the neutron channel residues. Observed enhancements in α-channel residues have been accredited to the coaction of CF+ICF mechanisms. The estimated α-channel $F_{\rm ICF}$ exhibits an increasing trend with bombarding energy. The variation of α-channel $F_{\rm ICF}$ with breakup threshold for the ^{6}Li and ^{7}Li reaction on ^{93}Nb indicates more $F_{\rm ICF}$ for the ^{6}Li reaction over ^{7}Li due to smaller S_α for ^{6}Li.

Research grant No. CRG/2018/002354 from SERB (IN) and a research fellowship from MHRD, Government of India, are gratefully acknowledged.

REFERENCES

[1] L.F. Canto *et al.*, *Phys. Rep.* **596**, 1 (2015).
[2] S. Santra *et al.*, *Phys. Lett. B* **677**, 139 (2009).

[3] F.A. Souza *et al.*, *Nucl. Phys. A* **821**, 36 (2009).
[4] H. Kumawat *et al.*, *Phys. Rev. C* **81**, 054601 (2010).
[5] M.R. Cortes *et al.*, *Phys. Rev. C* **108**, 054601 (2023).
[6] D. Chattopadhyay *et al.*, *Phys. Rev. C* **94**, 061602(R) (2016).
[7] A. Singh, M. Maiti, T.N. Nag, S. Sodaye, *Phys. Scr.* **98**, 025306 (2023).
[8] D. Kumar, M. Maiti, *Phys. Rev. C* **96**, 044624 (2017).
[9] P.K. Giri *et al.*, *Phys. Rev. C* **100**, 024621 (2019).
[10] M. Gull *et al.*, *Phys. Rev. C* **98**, 034603 (2018).
[11] P.K. Rath *et al.*, *Phys. Rev. C* **79**, 051601(R) (2009).
[12] M.K. Pradhan *et al.*, *Phys. Rev. C* **83**, 064606 (2011).
[13] C.Y. Wong, *Phys. Rev. Lett.* **31**, 766 (1973).
[14] `http://nrv.jinr.ru/nrv/webnrv/qcalc/`
[15] M. Herman *et al.*, *Nucl. Data Sheets* **108**, 2655 (2007).
[16] M. Blann, *Phys. Rev. C* **54**, 1341 (1996).
[17] A. Singh, M. Maiti, T.N. Nag, S. Sodaye, *Phys. Rev. C* **108**, 024607 (2023).